CEBAF PROPOSAL COVER SHEET

This Proposal must be mailed to

CEBAF
Scientific Director's Office
12000 Jefferson Avenue
Newport News, VA 23606

and received on or before OCTOBER 30, 1989

A. TITLE:

TWO-NUCLEON KNOCKOUT REACTIONS ON ^{3,4}He

B. CONTACT PERSON:

Richard A. Lindgren

ADDRESS, PHONE AND BITNET:

Dept, of Physics
University of Virginia
Charlottesville, VA 22901

Phone 804-924-6581
Fax 804-924-4576
BITNET RAL5@VIRGINIA

C. THIS PROPOSAL IS BASED ON A PREVIOUSLY SUBMITTED LETTER OF INTENT

☒ YES
☐ NO

IF YES, TITLE OF PREVIOUSLY SUBMITTED LETTER OF INTENT

88-03, 88-18, 88-41, 88-78

D. ATTACH A SEPARATE PAGE LISTING ALL COLLABORATION MEMBERS AND THEIR INSTITUTIONS

==

(CEBAF USE ONLY)

Letter Received_____ 10-31-89 _____

Log Number Assigned____ PR-89-030 ____

/___ KES _____

Contact: Lindgren

Two-Nucleon Knockout Reactions on ^{3,4}He

THE HALL A COLLABORATION

American University, Calif. State University LA, Case Western Reserve and LANL
CEBAF, George Washington University, University of Georgia, IUCF
Kent State University, University of Maryland, Massachusetts Institute of Technology
University of New Hampshire, National Institute of Science and Technology
Norfolk State University, University of Regina, University of Rochester
Rutgers University, University of Saskatchewan, Stanford University
University of Virginia, University of Washington, College of William and Mary
NIKHEF-K, CEN Saclay, University of Clermont-Ferrand
INFN Sezione Sanita, University of Lund

Spokespersons: M. B. Epstein (CSLA), R. A. Lindgren (UVa)
G. Lolos (U. Regina), Z. E. Meziani (Stanford)

ABSTRACT

We propose to study the two-nucleon knockout reactions (e,e'pp) and (e,e'pn) on ^{3,4}He as a preliminary investigation of two-body currents and correlations in nuclei. The ^{3}He nucleus is initially selected because it is the lightest non-trivial nuclear system where realistic wave functions are available. We plan to measure electron-proton-proton and electron-proton-neutron angular correlation cross sections in geometries where the kinematics may permit simplified interpretation of the data and that selectively emphasize various components of the knockout mechanism. We expect to observe signatures of three important effects that contribute to the knockout process, namely initial state short-range correlations, two-body meson exchange currents and final state interactions. We plan to carry out these measurements using the 1-4 GeV CW electron beam at CEBAF and the two high resolution spectrometers in Hall A for detecting electrons and protons. A third detector arm, a segmented plastic scintillator hodoscope, is being developed for detecting protons and neutrons. This third arm and a high power cryogenic ^{3}He target capable of luminosities L $= 10^{38}$ cm^{-2}s^{-1} will make these experiments feasible.

1. PURPOSE

We propose to investigate the two-nucleon knock-out (e,e′pp) and (e,e′pn) reactions on nuclei [3,4]He in regions of phase space where correlation cross sections are expected to be large. Three contributions to the knock out mechanism that are expected to be important are initial state short-range nucleon-nucleon correlations, two-body meson exchange currents, and final state interactions between the nucleons. Initially we plan to measure electron-proton-proton and electron-proton-neutron angular correlations cross sections in geometries where kinematics may permit simplified interpretation of the data and selectively emphasize various components of the knock out mechanism. Count rate estimates indicate that in particular geometries where the nucleons are expected to be highly correlated at moderate relative momenta in the initial state, it would be expedient to carry out these measurements in Hall A using the two high resolution spectrometers for the detection of the electron and the high momentum proton. The second proton in two of the three geometries will be detected using the segmented scintillation hodoscope being developed by NIKHEF. The neutrons will be detected in the large segmented plastic scintillator array under development at UVa. A pressurized, low temperature, high power cryogenic target capable of luminosities of 10^{38} cm^{-1} s^{-1} is being developed in collaboration with Cal State at LA and UVa.

2. SCIENTIFIC MOTIVATION

During the past 30 years inclusive elastic and inelastic electron scattering have been undeniably one of the most successful probes of the study of the structure of the nucleon and the nucleus. The effective interaction between the electron and the nucleus is taken to be the free electron-nucleon interaction, which is sufficiently weak compared to the strong interaction, that it can be accurately calculated by perturbation theory in quantum electrodynamics. In the simple picture of the electromagnetic interaction where a single photon is exchanged between the scattered electron and one nucleon, dipicted in Fig. 1a, nuclear structure effects can be cleanly separated from the reaction mechanism. As a result electron scattering has been a primary source of information on the structure of the nucleus. As electron scattering experiments probed higher momenta and have

become more sensitive to the details of the nuclear wavefunctions, the breakdown of the independent particle model of the nucleus and the above simple picture became more apparent. The need to include two-body meson exchange currents has been clearly demonstrated by high momentum elastic electron scattering studies on ^{2}H, and ^{3}He and in the threshold disintegration of ^{2}H. More recently, results from (e,e'p) experiments[1] have provided provacative evidence for the existence of new two-body effects such as correlated pairs in nuclei.

Measurement of these nucleon-nucleon correlations (Fig. 1b) will be very sensitive to the spatial structure of nucleon wavefunctions in the nucleus at distances smaller than the nucleon size where the internal structure of the hadrons can not be ignored. Conversely, measurements will be also sensitive to the high momentum components of the relative nucleon momentum in the nucleus, which is shown in Fig. 2 for ^{3}He. Obviously, such measurements will permit fundamental studies of the interplay of nucleonic, mesonic, and quark degrees of freedom in the nucleus. Precision information on short-range correlations will be most directly accessible through two-nucleon knockout (e,e'2N) reactions where the electron and two ejected nucleons are simultaneously detected. In the past such experiments were not feasible. The new continuous electron beam accelerator facility (CEBAF) provides the first opportunity to conduct the necessary triple coincidence three arm experiments. Such experiments will provide important and fundamental information on the elusive short range two nucleon correlations, two-body meson exchange currents, (Fig. 1c) and associated final state interactions between the ejected nucleons (Fig. 1d) and the nucleus.

A. Indirect Evidence For Nucleon-Nucleon Correlations

The lack of direct evidence for nucleon-nucleon correlations in nuclei is a longstanding unresolved problem in nuclear physics. However, the indirect evidence is tantalizing and gradually accumulating. For example, experimental results from (e,e')[2] and (e,e'p)[1,3] has provided indirect evidence on the importance of multi-body 2N and even 3N correlations in nuclei. The interpretation[4] of the (e,e') inclusive experiments in the quasi-elastic, dip, and Delta regions schematically shown in Fig. 3 suggest higher order processes not included in single nucleon

absorption. In the case of the $^{40}Ca(e,e')$ reaction[2], the separated longitudinal and transverse response functions shown in Fig. 4 exhibit much lower strengths than predicted by the independent particle models. Calculations including nucleon-nucleon correlations have been more successful[5]. There is an excess of experimentally observed strength in the dip region between quasi-elastic and the Delta region, over and above what was predicted by conventional models[6]. Results of calculations including both nucleons and quarks in the nucleus shown in Fig. 5 predict the dip region to be filled in by knockout of the correlated pn and pp pairs. Other calculations show that about half of the strength is due to meson exchange currents.[8] Conclusions from single arm experiments have basically reached their limits in constraining the physics in the quasi-elastic and Delta regions.

In exclusive $(e,e'p)$ experiments[1] such as on ^{3}He a broad peak shown in Fig. 6 was observed at missing energies suggestive that the virtual photon was absorbed on a pair of correlated nucleons. A similar effect has been observed in the study of the ^{12}C $(e,e'p)$ reaction[3]. One recent calculation[9] concludes that final state interactions (FSI) based on single nucleon absorption cannot account for the strength or the shape of the missing energy spectra in in ^{12}C (e,e'). Furthermore, not even 2-nucleon mechanisms can account for the data suggesting higher order processes such as 3-nucleon absorption.[9]

The 2-nucleon mechanism is most strongly supported by $(\gamma,2N)$ photoabsorption results in the Delta region with real photons, which emphasizes the quasi-deuteron nature of the absorption process.[10,11] However, in recent photodisintegration[12] of ^{3}He (γ,pp) in the delta region, the conclusion was that real photoabsorption on a pair was required to account for most of the data. Also calculations indicate the possibility of effects due to 3 body forces.

In addition to (e,e'), $(e,e'p)$ and (γ,NN) reactions pion absorption has provided us with a wealth of information of correlations effects. The pion and electron are complimentary probes in that the pion is a surface probe while the photon (long mean free path) is a volume probe. Similar to the real photon, the pion is absorbed predominantly on a T=0 pn pair due to the large momentum mismatch between the pion and the (outgoing) nucleon. However, the T=0 absorption channel

cannot account for more than 40% of the total absorption cross-section, including a very large (400%) correction for final state interactions (FSI.)[13] Subsequent investigations on ^{3}He and ^{4}He measured the 3-nucleon contribution[14]. The very latest results on the ^{12}C(π^+,pp)X reaction, however, indicate that the "pure" 2-nucleon absorption is in fact -40% of the total absorption cross-section at Tπ+=165MeV.[15] FSI would raise this ratio to the point that 2NA+3NA would account for almost ~90% of the total absorption cross-section.

B. Two-body Meson-exchange Currents (MEC) and Final State Interaction (FSI) Effects.

It was found necessary to introduce two-body meson-exchange and isobar currents in the electron-nucleus interaction when calculations based on one-body currents alone did not reproduce elastic electron scattering data on ^{2}H and ^{3}He as well as electrodisintegration of ^{2}H. These nuclei have established the clear need for the importance of including two-body currents, $\vec{J}_2$, in nuclei. In fact the existence of two-body potential, V, in the nucleus and current conservation requires that the existence of the relation $\vec{q} \cdot \vec{J}_2 = [V,\rho]$. Consequently, two body currents are simply a result of current conservation and a static two-body potential (eg. the one pion exchange potential). Despite previous successes there are important aspects of MEC that are still open to question[16]. Certainly, the determination of the two-nucleon densities is required for accurate calculations. The strong model dependence of the pion-nucleon-nucleon vertex, the off shell nature of the nucleon form factor, and the kinds of mesons that need to be included, and relativistic effect all need further study. We expect that studies of the (e,e′pn) reaction, where MEC effects are not negligible and comparison with (e,e′2p) would emphasize and place constraints on the physics necessary to describe these dynamical correlations.

Definitive test on our understanding of final state interactions is lacking. It will be extremely important to account for such effects if we are to reliably extract two-nucleon correlation functions. It is hoped that by choosing different geometries such as parallel and antiparallel kinematics in (e,e′pp) on ^{3}He that we can disentangle FSI between the ejected protons themselves and between the ejected proton and the spectator neutron as well as separate these effects from initial state

correlations and MEC. By measuring cross sections over a range of outgoing proton energies particularly near 200 MeV, where there is a minimum in the central force component in the nucleon-nucleon interaction, we may be able to turn on or turn off the dominant FSI effects.

3. PROPOSED EXPERIMENT

We propose to measure electron-proton-proton (e,e'pp) and electron-proton neutron (e,e'pn) triple coincidence cross sections on ^{3}He and ^{4}He. The first measurements will be on ^{3}He, the lightest non trivial nuclear system, where accurate three body wave functions from the Fadeev equations are available for the bound state and good approximate wave functions are available for the continum. Because we have a good handle on the wavefunctions, we have the best chance to identify initial state nucleon-nucleon correlations in the data and to separate out the effects of MEC and FSI from the correlations. The follow-up studies on ^{4}He will be useful in obtaining systematics, particularly with regard to FSI between the emitted proton and the 2 spectator nucleons as opposed to 1 in ^{3}He.

We have chosen three kinematic geometries in regions of phase space where the cross sections are expected to be large, and where the description of the knock-out process is simplified. We consider it important to study both (e,e'pp) and (e,e'pn) because each selectively emphasize different contributions to the cross section and probably both of these measurements can be made simultaneously. Our first priorty will be the study of initial state short range correlations using the (e,e'2p) reaction because it appears to be a clearer and simpler probe since MEC and delta production are suppressed. On the other hand cross sections are larger in (e,e'pn) and may be a richer probe of the physics because it can provide information on both MEC and delta-nucleon correlations as well as ground state correlations. Real photoabsorption[17] (γ,pp) and (γ,pn) in the delta region show that pn is about 20 times stronger than pp. Furthermore, electron scattering provides information on the q dependence of the two-nucleon process in the delta and dip region where pn pairs are expected to be responsible for the excess strength.

We have estimated count rates in (e,e'2p) an ^{3}He assuming the virtual photon is absorbed on a single proton of a correlated pair as shown in Fig. 1b. The longitudinal cross section for this process has been calculated[18] in the PWIA using a code provided by Laget. We do not include

rescattering of the two protons or final state interactions and the residual neutron is treated as an inert spectator with zero momentum. Since the residual neutron is in a relative s, state with respect to the pair, maximum cross sections are expected when $p_n=0$. We have used this simple model to find regions of phase space where the results are interesting, the cross sections are measurable, the emitted protons have sufficient energy to be detected, and the three detectors do not get in each others way.

We have considered three different geometries for (e,'e2p). We first consider the situation where the two protons are emitted back to back in the laboratory (antiparallel), emitted in the same direction (parallel), and where the two protons are emitted symmetrically with the absorbed virtual photon bisecting the angle between the ejected protons. Specific geometries for each case are shown in Fig. 7. In each case the initial momentum of the pair is zero in the laboratory, the neutron behaves as a spectator, the virtual photon is absorbed on one nucleon, and the center of mass of the pair lies along q.

A. ^{3}He (e,e'2p)

1. Two protons emitted back to back. (anti-parallel)

Before the collision the two protons are assumed to have opposite and equal momenta as dipicted in Fig. 7. After the photon is absorbed by one of them, they are ejected back to back or 180° apart in the laboratory. This geometry has the advantage of minimizing final state interactions between the ejected protons since they leave in opposite directions. Using the model previously described, cross section calculations for various electron bombardment energies 1-4 GeV at electron scattering angles of $\theta=8°$, 15°, and 22° are performed. These angles are chosen because each is the minimum angle achievable with the expected electron angular acceptance of 4.9, 8.0 and 15.6 ms depending on the position of the two quadrupoles of the high resolution spectrometer[19]. The calculated cross sections as a function of the electron energy loss ω, are shown in Fig. 8 and as a function of initial proton momenta, P_i, in Fig. 9.

At E_o = 2 GeV, θ_c = 8°, we see from Fig. 7 that the proton that absorbed the photon is

emitted at 41° along q with momentum 574 MeV/c and the backward going proton emitted at 131° has momentum 242 MeV/c with kinetic energy of 31 MeV. We plan to detect and momentum analyze the high momentum electron and proton with the two high resolution spectrometers in Hall A with momentum resolution typically of the order 10^{-3}. The low energy proton will be detected in the segmented scintillator hodoscope being designed by the NIKHEF group. For (e,e'pn) the backward going neutron is detected in a segmented plastic scintillator hodoscope being developed at the University of Virginia. Both detectors are discussed in more detail in the next section A typical arrangement of the spectrometers and scintillator arrays are shown in Fig. 10. Estimated triple coincident count rates are shown in Table 1. The rate varies from 17771 counts/hr to 63 counts/hr depending on various factors but is mainly dependent on the initial momenta sampled in ^{3}He. We see from Fig. 9 that this geometry limits our sampling of initial momenta from P_i = 250 MeV/c to P_i = 500 MeV/c. At the low momentum end the energy of the backward moving proton is too low and on the high end the cross section is too small.

Count rate calculations assumed a luminosity of $\mathcal{L}$ = 1.7 x 10^{37}cm^{-2}s^{-1} corresponding to 20 μa of beam on a high pressure ^{3}He gas target of density 0.75 cm/cm^2. If accidentals are not a problem, higher luminosities (10^{38}) could be achieved with the high power 3He target that is under development and, therefore, lower cross sections could be measured.

2. Two protons are emitted in the same directions. (parallel)

In this case the two protons are ejected from the nucleus in the same directions and are detected in the same spectrometer. This particular kinematics is very sensitive to final state interactions between the two protons since the relative momenta is so small and, therefore, is complementary to the antiparallel case. Where FSI is expected to be minimal unfortunately, Figs. 11 and 12 show that only initial momenta below 250 MeV are sampled corresponding to kinetic energies below 30 MeV. Although Table 1 shows that for momenta near 250 MeV/c, the rates are reasonable, 2000 → 4000 counts/hr. Above 250 MeV/c kinematics are not feasible at the angles shown in Fig. 11.

3. Two protons are emitted symmetrically with respect to the direction of the virtual photon. (symmetric)

This geometry has the advantage that both protons have the same momentum before and after the collision. This means that there is no ambiguity in the samping of momenta in the correlation function, which is directly proportional to the cross section in PWIA. In the other two geometries two protons of two different initial momenta were being sampled, which correspond to two indistinguishable protons of the same energy detected in the spectrometer.

The electron energy loss spectrum is shown in Fig. 13 and the cross section as a function of the proton initial momentum P_i is shown in Fig. 14. These results show that particularly at $\theta_i = 8°$, cross sections are favorable in accessing momenta from P_i=300 MeV/c, to about 900 MeV/c corresponding to rates from 5765 to 63 counts per hour. Note that the lowest energy proton in this geometery from Table 1 is 46 MeV and the separation angles between the two protons is suitable to accommodate the high resolution spectrometer and scintillator hodoscope. Since it is the relative momenta between the two protons in the initial state that is important, these kinematics permit us to probe relative momenta from 600 MeV/c up to 1800 MeV/c.

B. ^{3}He(e, e'pn)p

It is well known from photoabsorption experiments that (γ,pn) cross sections are about 10-20 times larger than (γ,pp) in the delta region. Also PWIA calculations[18] previously described indicate that the transverse (e,e'pn) cross sections are significantly larger than the transverse or longitudinal (e,e'pp) cross sections as shown in Fig. 15. The formation of the delta and exchange currents dominate in (e,e'pn). Consequently, the pn reaction is not as ideally suited to study initial state correlations, but is more suited to the study at meson-exchange current induced correlations and delta-nucleon correlations in the delta region. Using the same geometry and kinematics as previously indicated, cross sections are expected to be 10 → 100 times larger. The segmented scintillator array planned to detect neutrons will also have the an angle of 40 ms comparable to the proton detector and a neutron detection efficiency of about 20%. Hence, typical count rates for ^{3}He (e,e'pn) may be expected to be 2-20 times higher than the (e,e'2p) reaction. Using the mass

dependent empirical formula for estimating (γ, p) cross sections and using the ^9Be (γ, pp) and ^9Be (γ, pn) angular correlation data[17] shown in Fig. 16, we have estimated the tramsverse $(e, e'pn)$ cross section at low q for ^3He in back to back kinematics. A plot of the count rate versus electron beam energy for several different q's, where the proton is detected in the direction of q and the neutron is detected at the peak of the pn angular correlation is shown in Fig. 17. At E=2 GeV, the count rates are a few thousand per hour typical of the $(e, e'2p)$ in Table 1. The large segmented neutron detector is presently being constructed at UVA for $^3He(\gamma, pp)n$ and $^3He(\gamma, pn)p$ studies using polarized 300 MeV photons at the LEGS facility at Brookhaven National Laboratory. We plan to carry out the experiment in the spring 1990. This system will be redesigned with appropriate shielding for detecting neutrons in the electron beam environment at CEBAF.

C. Singles and Accidental Coincidences Rates

Preliminary calculations of the electron singles rates with a 2 GeV electron beam at $\theta = 8°$ with angular and momentum acceptances and luminosities used to estimate triple coincident count rates at electron energy losses above the quasielastic peak are about 0.5 MHz. Including the quasielastic peak increases the rate by about a factor of ten.

The singles rates in the proton spectrometer at $\theta = 45°$ with a 10% momentum acceptance centered about 400 MeV/c was estimated to be about 1 MHz.

Further work is in progress in determining singles rates in the electron and proton spectrometer and in the NIKHEF proton and UVA neutron scintillator hodoscopes. Calculations of the threefold accidental rates at this time and the accidentals from double arm real coincidence with singles rates in the third detector is also in progress.

4. THIRD ARM DETECTOR DEVELOPMENT

A. Proton Detection System

For the detection of protons we intend to use an updated version of the NIKHEF-K hadron detector. This will be a 200 msr upgrade of the current 40 msr detectors. The new detectors are designed to have a dynamic range for proton detection that extends from 35 to 250 MeV. Fig. 18 is a schematic drawing of the present detector. It is a segmented and lamanated array of plastic

scintillators consisting of five counter layers plus a vertical a horizontal hodoscope (also plastic). The angular resolution is determined by the hodoscopes and is 0.5 degrees when operated at a distance of 0.75 m from the target. All the Photo tube analog signals are digitized by NKHEF developed frontend modules. The electronics operates in a VME environment and are monitored and controlled by a SUN workstation.

The energy of the particles is determined by summing the adc's of all the counters along the particles trajectory. Preliminary results suggest a resolution of approximately 5 MeV for 100 MeV protons.

The detector has been operated at luminosities of 50 mg microA/cm^2 in a 1% duty cycle environment. it should be possible to use a luminosity of $6x10^{36}$ 3He atoms/cm^2 at 100% duty cycle as this would yield the same instantaneous count rate.

Figure 18 also shows a coincidence timing spectrum obtained from a ^{12}C(e,e'p) measurement which was performed in the quasi elastic region. The timing resolution of approximately 3 ns can be improved as no flight time corrections have been applied for the protons. The good real to random ratio demonstrates the ability of the first level trigger to discriminate protons from other charged particles.

The updated device will be built on the same principles as the current detectors although the possibility of using wire chambers or scintillating fibers instead of the hodoscopes is being investigated.

B. Neutron Detection

Neutrons will be detected using a segmented scintillator hodoscope currently under construction for studies of ^{3}He (γ,pn) and ^{3}He (γ,2p) reactions at the LEGS facility at BNL.

Currently our system consists of 32 scintillator bars. Each bar measures 10 cm x 10 cm x 160 cm and has light pipes and 2-inch photomultiplier tubes at each end to collect sufficient light for accurate particle time-of-flight measurements and to enable position determination along the 160 cm length. The large number of bars enables a variety of configurations to be set up with good angular coverage, and still provides a neutron detection efficiency of up to 30%. See Fig. 10 for a typical

arrangement of the bars in the two groups of 4x4 arrays. We also have 16 scintillator paddles, each measuring 0.6 cm x 11 cm x 160 cm, used to veto charged particles. Pulse height and timing signals are digitized using CAMAC ECL modules. Our data acquisition system is based on the LAMPF Q system, using an MBD. Detector support apparatus are currently under construction at University of Virginia. We eventually plan to increase the number of bars to 48. A detailed description including electronic logic is available.

The segmented scintillator hodoscope for detecting neutrons at CEBAF will require some level of shielding. Presently, various shielding materials and geometries are being considered. Monte Carlo calculations of the energy deposition in the scintillator from gamma rays, neutrons, and electrons are being studied. This work is being done in collaboration with Craig Wuest of Lawrence Livermore National Laboratory. Experimental test are also being considered.

5. TARGET CONSTRUCTION

Targets for this experiment and related experiments are being designed currently. These designs call for cryogenic gas targets to be operated at high pressure. Design concerns that have been addressed for these targets have included the high densities required to achieve luminosities of $10^{38}cm^{-2}s^{-1}$, the large amounts of heat deposited by the beam in the target, the high energy densities at the interaction region due to the small size the beam spot, the containment of density fluctuations due to beam heating and minimizing the thickness of target cell windows.

A preliminary design for a ^{3}He cell specifies a minimum operating temperature of 10 K and pressure of 70 atm. The corresponding target gas density is 0.17 g/cm^3. For an effective cell length of 10 cm (perpendicular) luminosities of $10^{38}cm^{-2}s^{-1}$ can be achieved for beam currents of 50-150 μA. For a cylindrical cell of 15 cm (physical) length with spherical end caps, a wall thickness of 0.03 cm of aluminum 7075-T6 is being incorporated in the current design. This design specifies that the target cell be viewable by two spectrometers simultaneously (one on each side of the beam) over an angular range of 10° - 130° in the scattering plane and 0° -± 10° in the scattering plane.

The bulk power dissipation in the target will be dealt with a LHe-4 refrigerator and a suitable

heat exchanger. For the ^{3}He target cell described previously, a maximum power dissipation of 1.2 kW (for a 150 μA beam) is anticipated. To minimize density variations due to local beam heating it is necessary that the target gas flow past the beam. Current preliminary designs specify a gas flow perpendicular to the beam direction at velocities as high as 30 m/s (for ^{3}He) assuming a tolerable density variation of no more than 20% for a minimum beam spot size of 0.1 mm. Experience in other laboratories, e.g. SLAC, indicates that such velocities are realized. For a 10% density variation, these velocities are roughly doubled, though they can again be reduced substantially (by more than a factor of two) if the beam is defocused or rastered. For example, it appears that it will be possible for the beam to be defocused to 1-2 mm horizontally which reduces the flow velocities needed by at least a factor of five.

Presently, a collaboration between groups from California State University, Los Angeles and the University of Virginia is involved in the design of these targets in collaboration with John Mark, a target specialist from SLAC.

6. BEAM TIME ESTIMATE

The amount of beam requested is based on the count rates in Table 1. We also have assumed that we wish to observed electrons with energy losses up to $\omega = 1$ GeV at incident energies of 2 and 4 GeV permitting full coverage of the interesting regions of the Bjorken scaling variable x. We also wish to observe the complete proton spectrum for each 10% byte in electron energy is the electron spectrometer. Assuming 10% bytes in proton spectrometer this corresponds to 40 different bytes in the antiparallel geometry. Using average counts rates of 4.0 counts/hr/MeV and assuming we wish to accommodate 100 counts/MeV, this would require 25 hours of beam for each byte or a total of 1000 hours for 40 bytes. Similar calculations for the parallel and symmetric geometries yield the results in Table 2. According to this calculation the amount of running time is 2050 hours. Adding 50% for set-up time, testing and contingency brings the total request for time to 3075 hours. If the detectors can operate at the fully designed target $\mathcal{L} = 10^{38}$cm^{-2}s^{-1}, then the total amount of hours reduces to 1809 hrs.

References

1. C. Marshand et al., PLB153 (1985) 29

2. Z. E. Menziani et al., PRL54 (1985) 1233

3. R. W. Lourie et al., PRL56 (1986) 2364

4. H. J. Pirner and J. P. Vary, PRL46 (1981) 1376, D. Day et al., PRL (1979) 1143

5. B. Frois andC. N. Papanicolas, Ann. Rev. of Nucl. and Part. Sci. 37 (1987) 133

6. J. Koch et al., NPA435 (1985) 765

7. P. M. Mulders, NPA459, 525 (1986)

8. J. W. Van Orden Et al., Annals of Physics 131 (1981) 451

9. J. S. O'Connell et al., PRL53 (1984) 1627

10. J. Arends et al., PRLB146 (1984) 303

11. P. Carlos et al., NPA431 (1984) 573

12. N. D'Hose et al., PRL63 (1989) 856

13. A. Altman et al., PRC34 (1988) 1986

14. G. Backenstoss et al., PRL61 (1985) 923

15. Z. Papandreou, Ph.D. Thesis, Univ. of Regina, August, 1989 (unpublished)
    Z. Papandreou et al., PRL (to be published)

16. D. Drechsel et al., Reports on Progress in Physics 52 (1989) 1083

17. M. Kanazawa et al., PRC 35 (1987) 1828

18. J. M. Laget, PRC 35 (1985) 832

19. J. Le Rose, CEBAF, private communication

List of Figures

Table 1. Sample count rates assuming the recoil neutron to be at rest, an electron and hadron spectrometer momentum acceptance of $\Delta p/p = 10\%$, a luminosity of 1.8×10^{37} cm^{-1} sec^{-1}, and detector solid angles of:

$$\Delta\Omega_e\ (\ 8°)\ \ = 4.9\ \text{msr}$$
$$(\ 15°)\ = 8.1\ \text{msr}$$
$$\Delta\Omega_{p_1}\ \ \ \ \ = 16.0\ \text{msr}$$
$$\Delta\Omega_{p_2}\ \ \ \ \ = 40.0\ \text{msr}$$

E_e (GeV)	ω (MeV)	θ_e	p_1 (MeV/c)	θ_1	T_1 (MeV)	p_2 (MeV/c)	θ_2	T_2 (MeV)	Q^2 ([GeV/c]^2)	x	$\dfrac{d^5\sigma}{\left(\frac{\text{pb}}{\text{sr}^3[\text{MeV/c}]^2}\right)}$	rate (hr^{-1})
anti-parallel												
2	200	8	574	-49.0	162	242	131.0	31	0.070	0.19	20.068	17771
1	200	8	540	-28.2	144	304	151.8	48	0.016	0.04	0.388	192
4	400	8	901	-49.0	363	238	131.0	30	0.280	0.37	6.126	10651
2	900	8	1424	-9.5	767	501	170.5	125	0.043	0.03	0.056	63
parallel												
2	78	15	274	-73.9	39	244	-73.9	31	0.262	1.79	1.304	2055
4	90	8	309	-76.8	50	250	-76.8	33	0.304	1.80	2.334	4635
4	280	15	558	-67.1	153	488	-67.1	119	1.014	1.93	0.011	65
symmetric												
2	100	15	298	-42.0	46	298	259.0	46	0.259	1.38	0.331	630
2	300	8	544	31.9	146	544	254.5	146	0.066	0.12	3.069	5765
4	300	15	544	-50.6	146	544	-81.5	146	1.009	1.79	0.012	83
4	700	8	877	28.4	346	877	267.4	346	0.257	0.20	0.109	639

.

Table 2. Beam times Estimates

Geometry	Ave Cts/Hr.	Ave Binwidth MeV	$\dfrac{\text{Cts}}{\text{Hr}-\text{MeV}}$	Total Bytes	$\dfrac{\text{Hrs.}}{\text{Byte}}$	Hrs.
Antiparallel	1000	250	4.0	40	25	1000
Parallel	2000	300	6.5	30	15	450
Symmetric	2000	300	6.5	40	15	600

Total hours	2050
Contingency	1025

$\mathscr{L} = 1.7 \times 10^{37} \text{cm}^{-2}\text{s}^{-1}$ Total Request   3075 hrs.

$\mathscr{L} = 10^{38} \text{cm}^{-2}\text{s}^{-1}$ Total Request   1809 hrs.
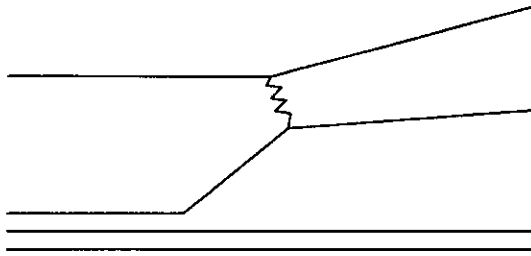
1a - ONE BODY
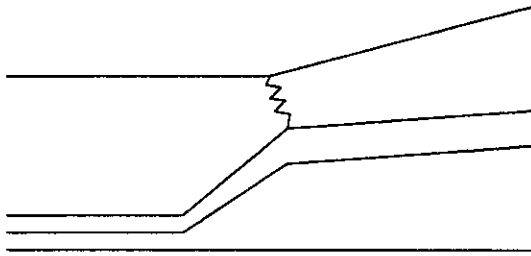
1b - CORRELATED PAIR
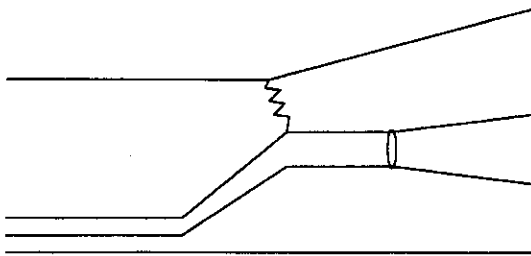
1c - FINAL STATE INTERACTIO
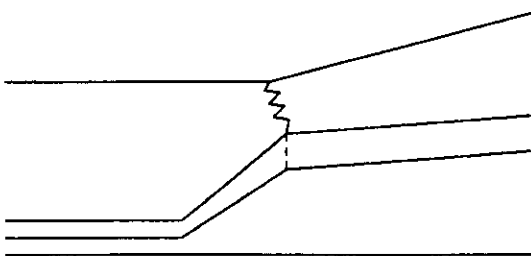
1d - MESON EXCHANGE CURREN

Fig. 1
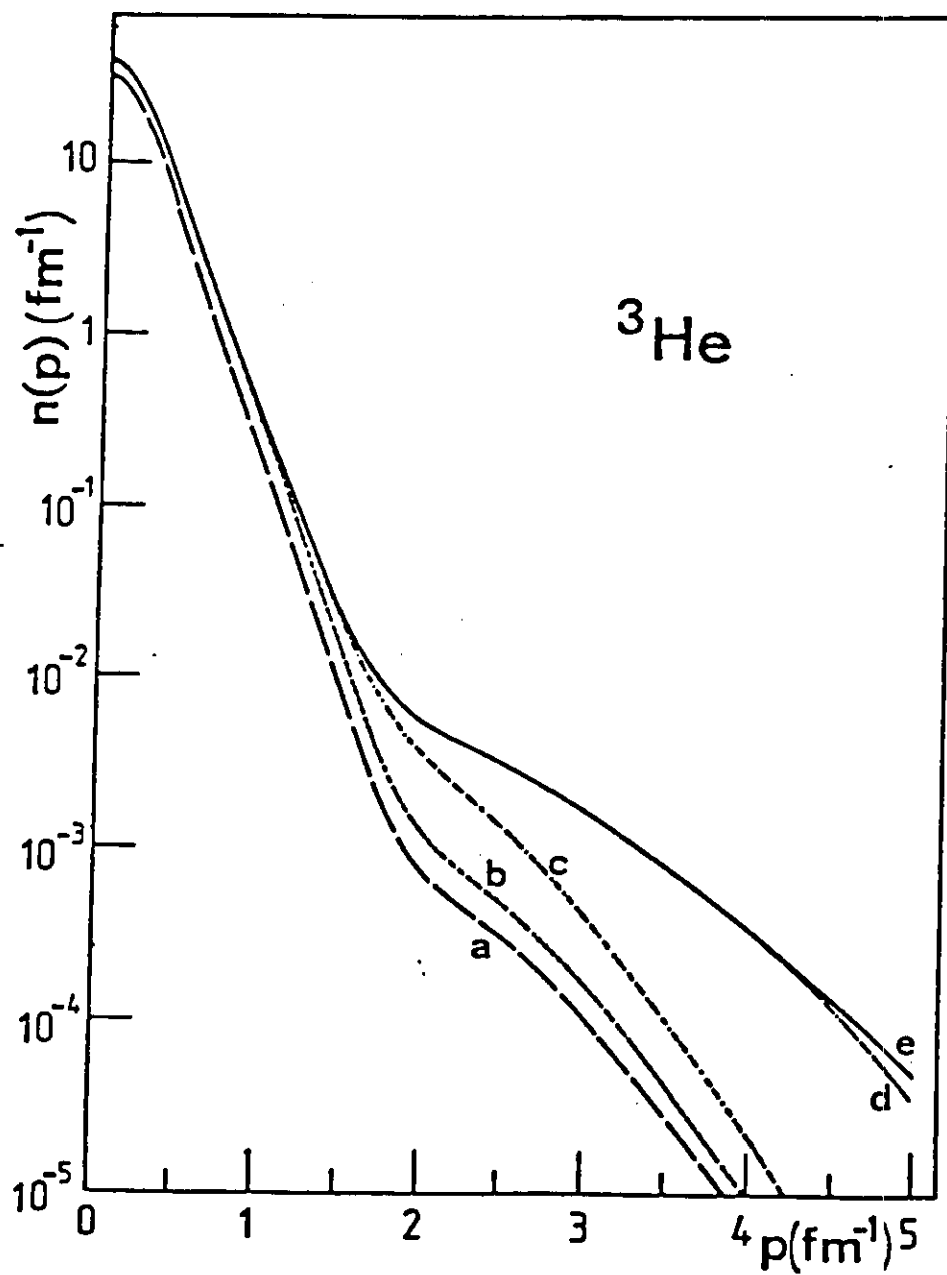
Fig. 2
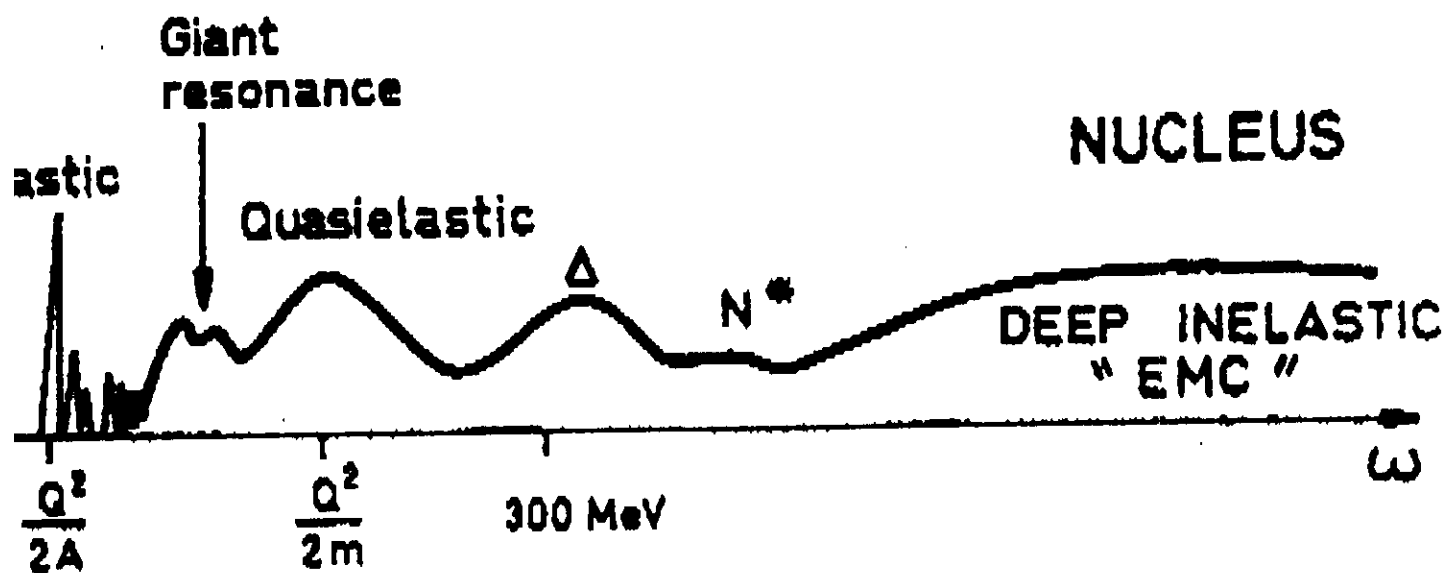
Fig. 3

Fig. 4

Fig 5

Fig. 6

PARALLEL

$\mathcal{E}_e = 2\ GeV$

79°

$q = 518$

$P_2 = 244$ $P_1 = 244$

$\mathcal{E}_e' = 1.922\ GeV$

15°

$P_2' = 244$ 79°

$P_1' = 274$

ANTI - PARALLEL

$\mathcal{E}_e = 2\ GeV$

49°

$q = 332$

$P_2 = 242$ $P_1 = 242$

$P_2' = 242$ 131° $\mathcal{E}_e' = 1.8$

8°

49°

$P_1' = 574$

SYMMETRIC

$\mathcal{E}_e = 2\ GeV$

71°

$q = 519$

$P_2 = 298$ 101° $P_1 = 298$

$\mathcal{E}_e' = 1.4\ GeV$

15°

42°

101°

$P_2' = 298$ $P_1' = 298$
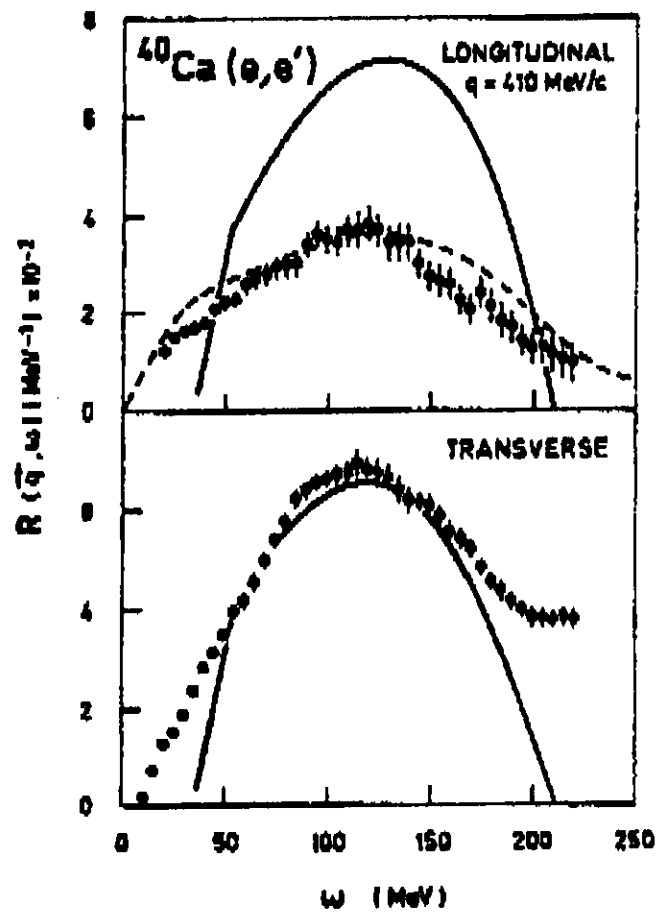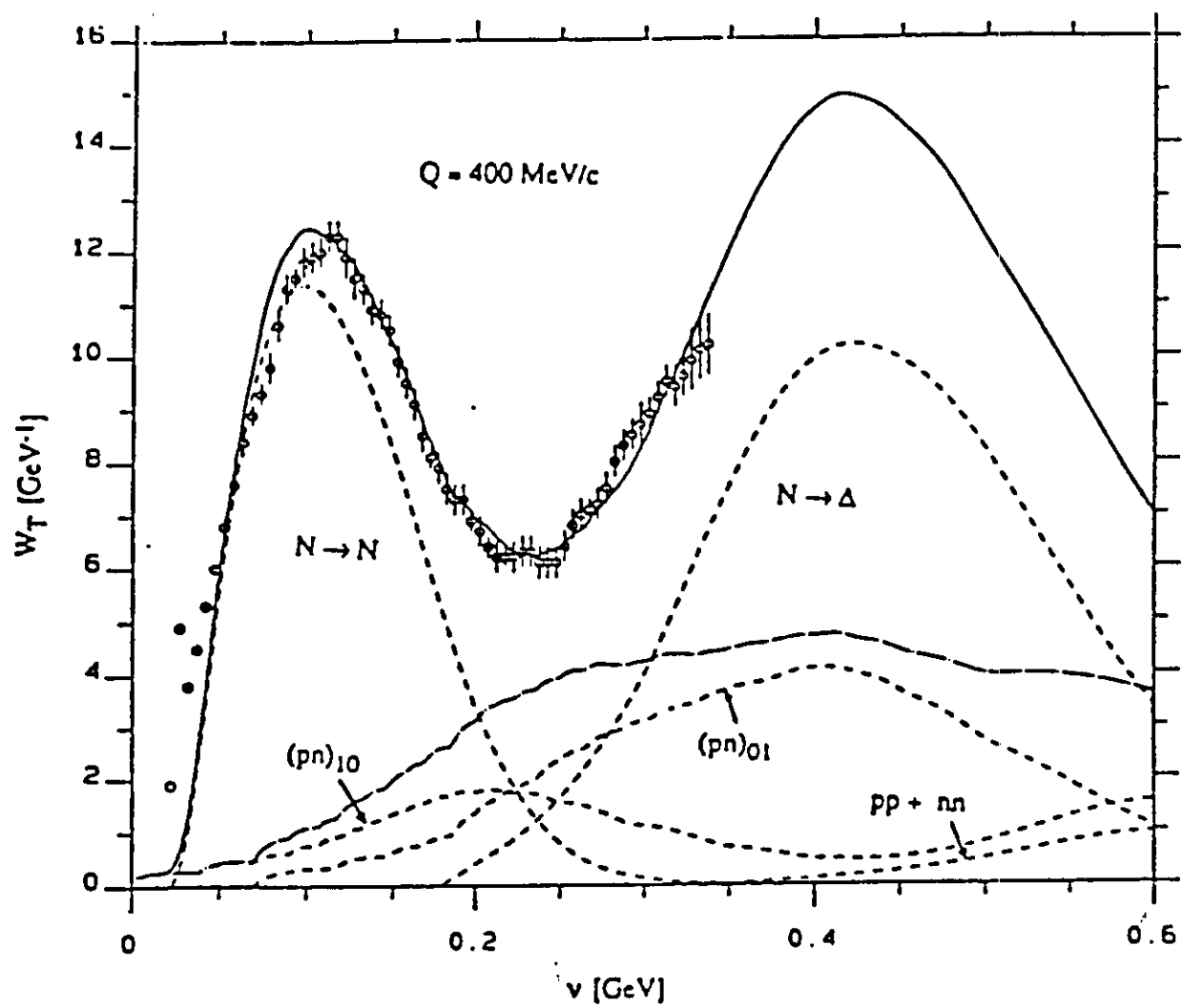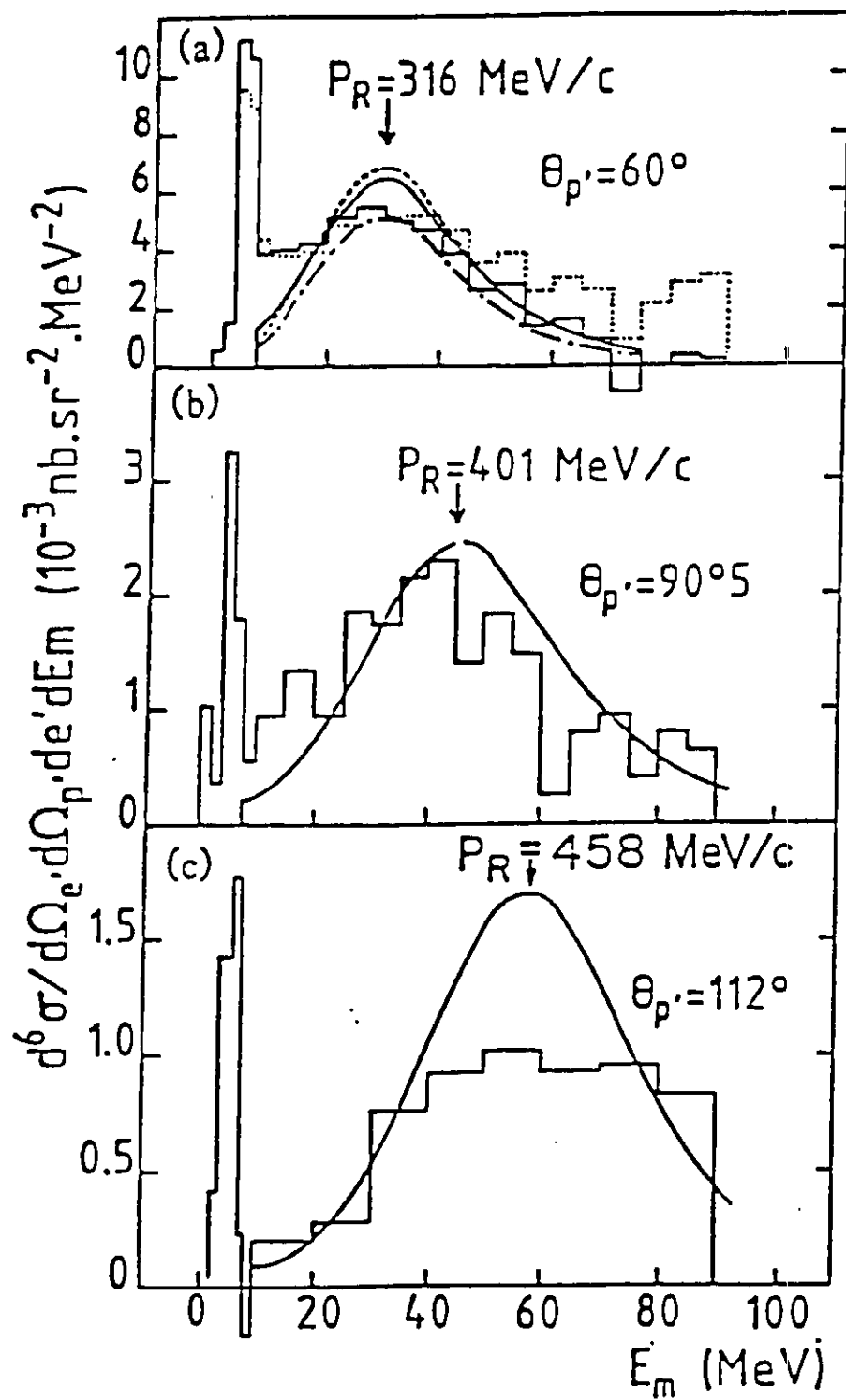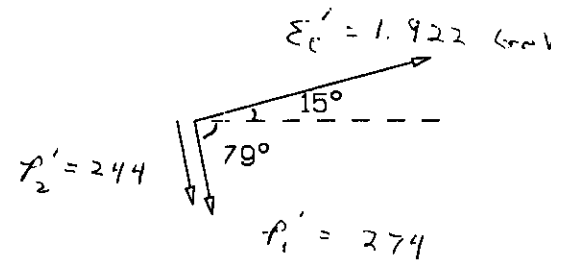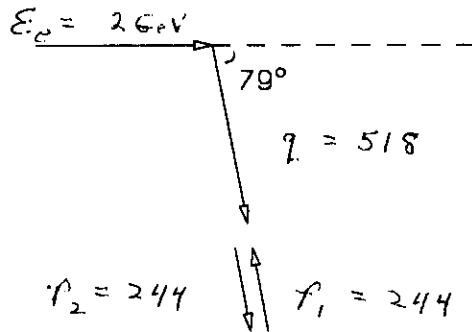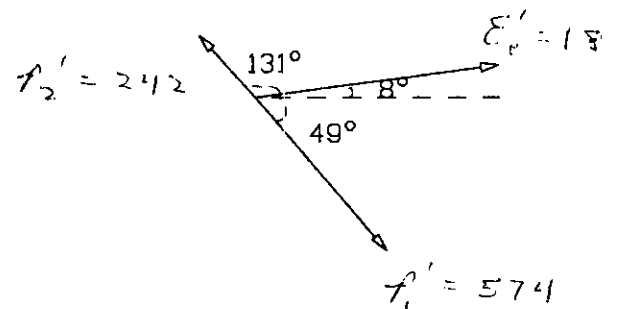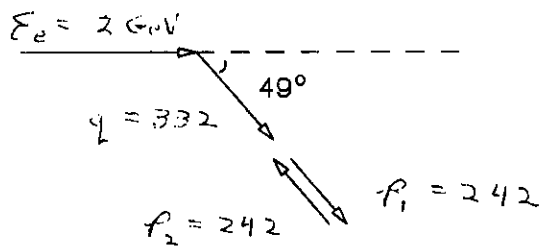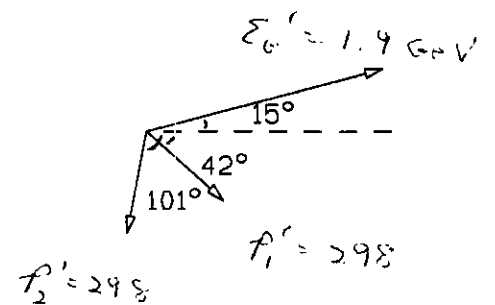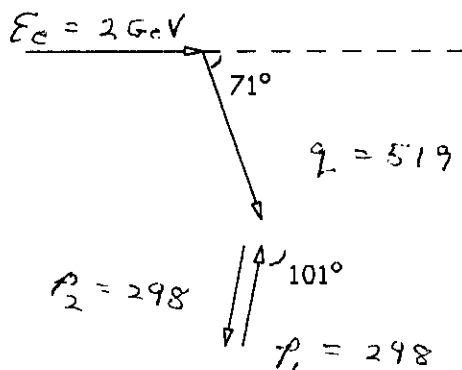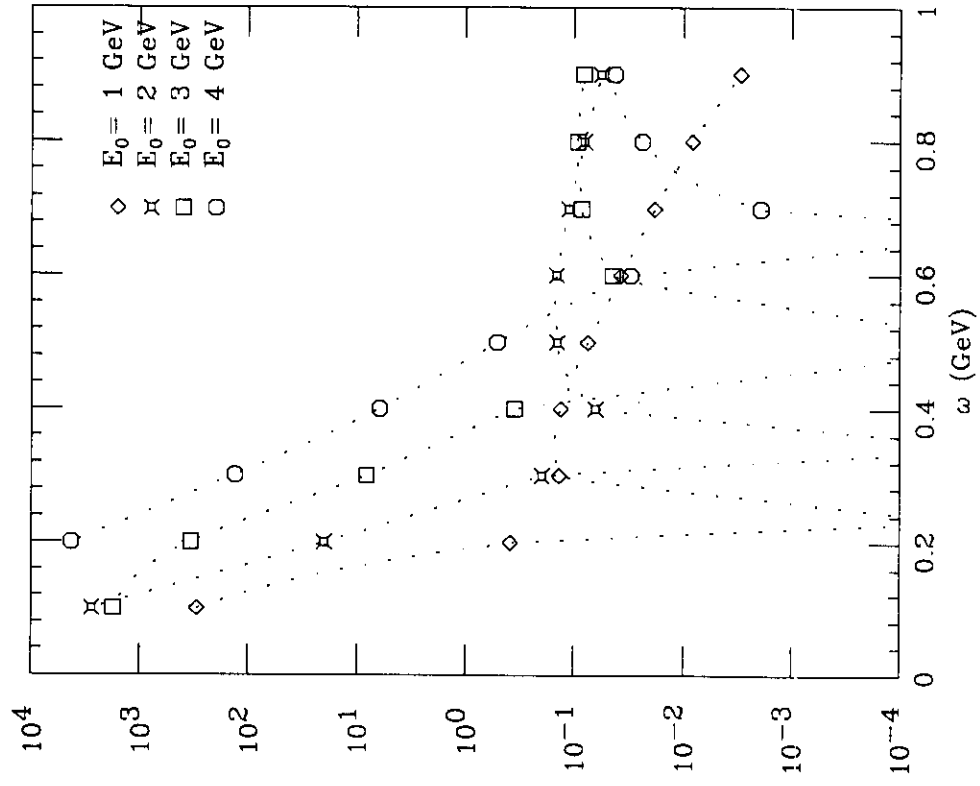
Fig. 8

$E_0 = 2$ GeV $\quad \theta_{cm} = 0°\quad$ anti-parallel

$$\frac{d^5\sigma}{d\Omega_e\,d\Omega_{p_1}\,d\Omega_{p_2}\,dp_e\,dp_1}\quad [\text{pb/sr}^3/(\text{MeV/c})^2]$$

P_i (MeV)

	θ_e	$= 8°$
θ_e	$= 15°$
θ_e	$= 22°$

$\theta_e = 8°\quad \theta_{cm} = 0°\quad$ anti-parallel

P_i (MeV)

$\diamond$	$E_0 = 1$ GeV
$\bowtie$	$E_0 = 2$ GeV
$\square$	$E_0 = 3$ GeV
$\bigcirc$	$E_0 = 4$ GeV

Fig. 6
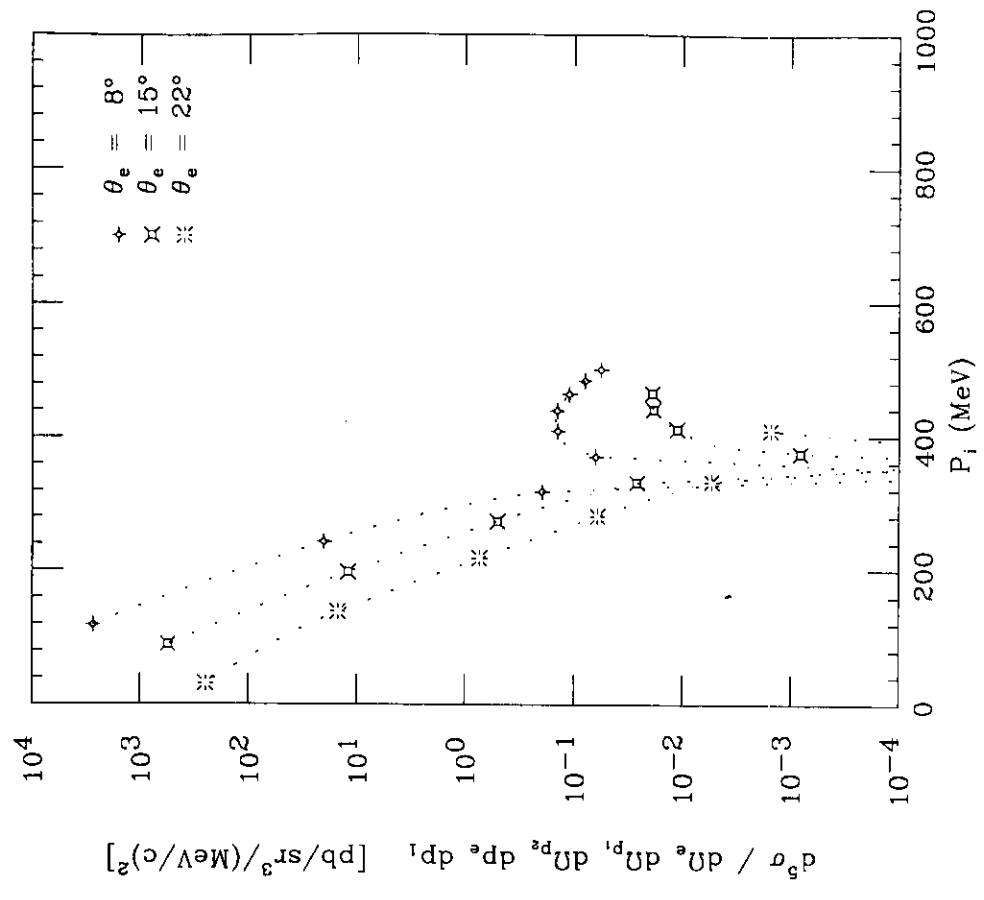
Proton Detector
or
Neutron Detector
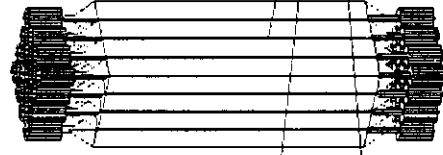
Electron Spectrometer

Proton Spectrometer

Target

e

P_2

P_i

Fig. 10

$E_0 = 2$ GeV $\theta_{cm} = 0°$ parallel

$\theta_e = 8°$
$\theta_e = 15°$
$\theta_e = 22°$

ω (GeV)

$d^5\sigma / d\Omega_e\, d\Omega_{p_1}\, d\Omega_{p_2}\, dp_e\, dp_1$ [pb/sr^3/(MeV/c)^2]

$\theta_e = 8°$ $\theta_{cm} = 0°$ parallel

$E_0 = 1$ GeV
$E_0 = 2$ GeV
$E_0 = 3$ GeV
$E_0 = 4$ GeV

ω (GeV)

$\theta_e = 8° \quad \theta_{cm} = 0° \quad parallel$

$E_0 = 2 \, GeV \quad \theta_{cm} = 0° \quad parallel$

$d^5\sigma \,/\, d\Omega_e \, d\Omega_{p_i} \, dp_e \, dp_i \quad [pb/sr^3/(MeV/c)^2]$

Fig. 12

Fig. 13

$\theta_e = 8°$ $\theta_{cm} = 90°$

$E_0 = 2$ GeV $\theta_{cm} = 90°$

Fig. 14

Fig. 15

$^9Be(\gamma, pn)$
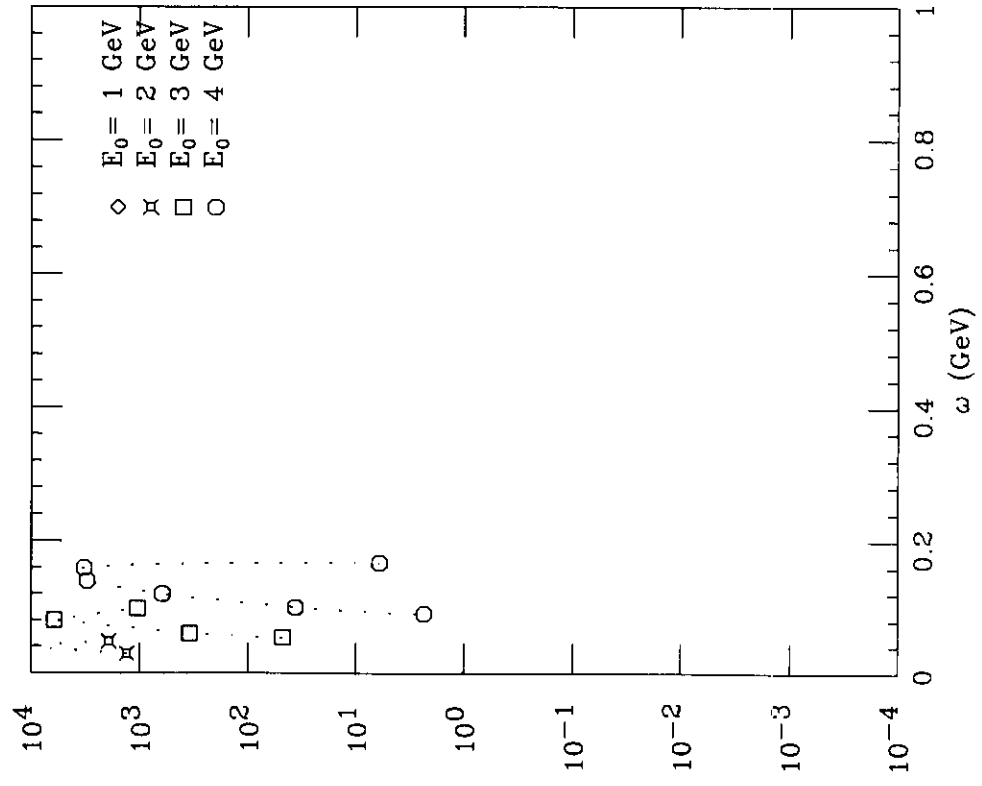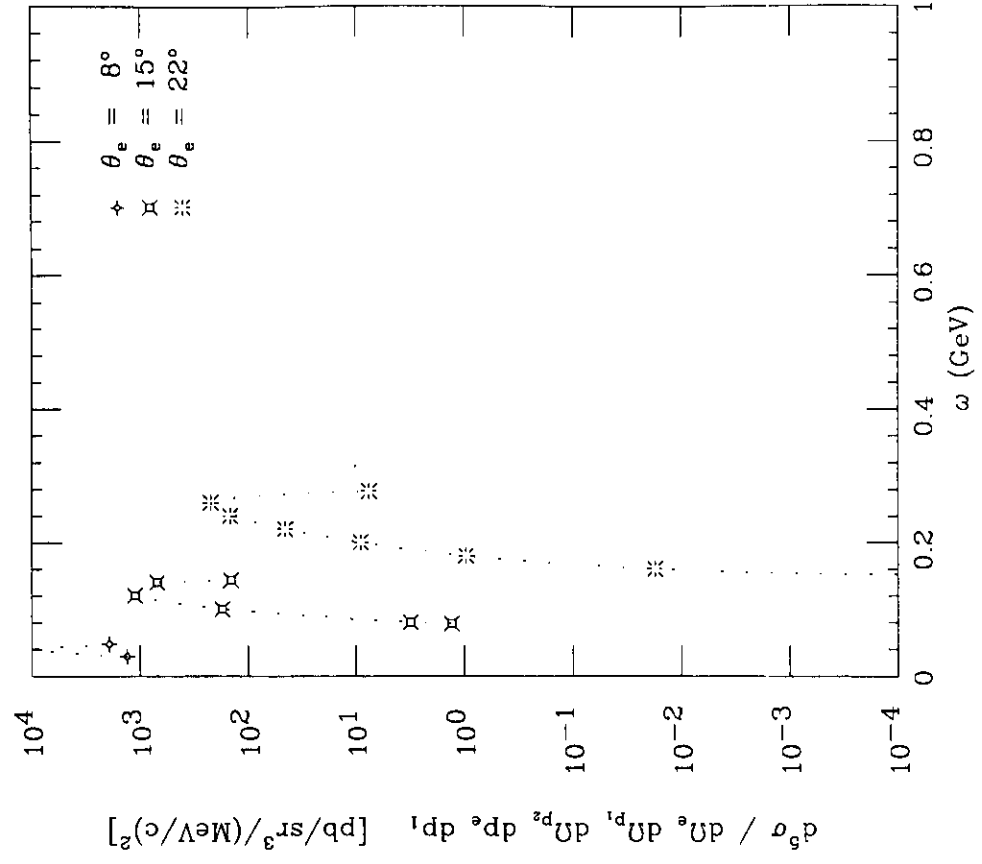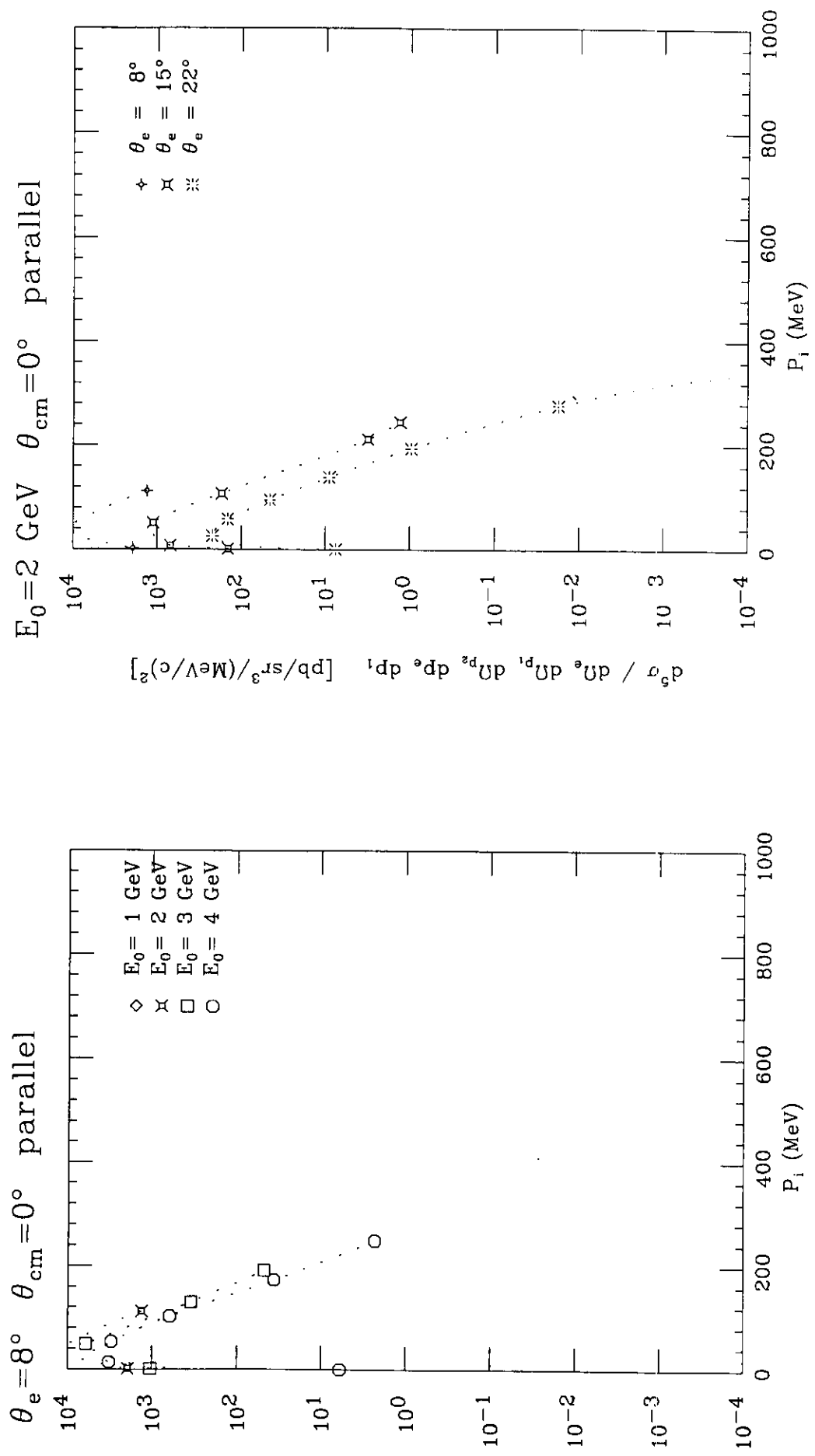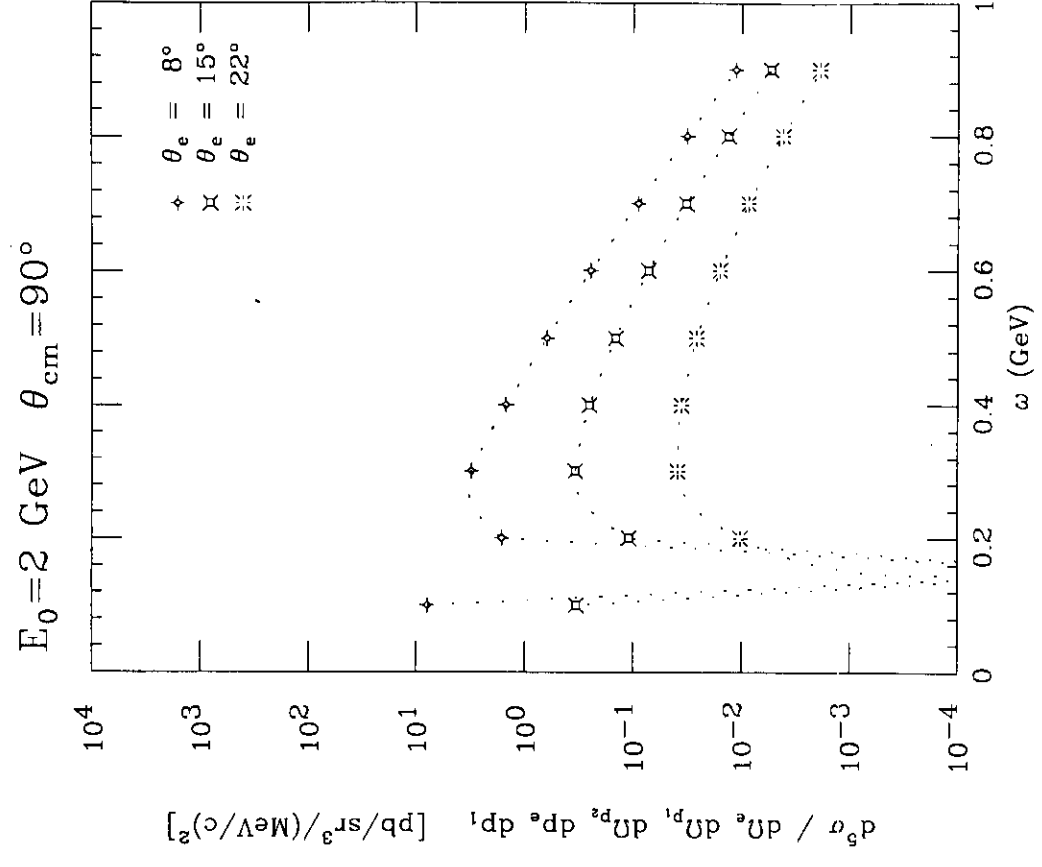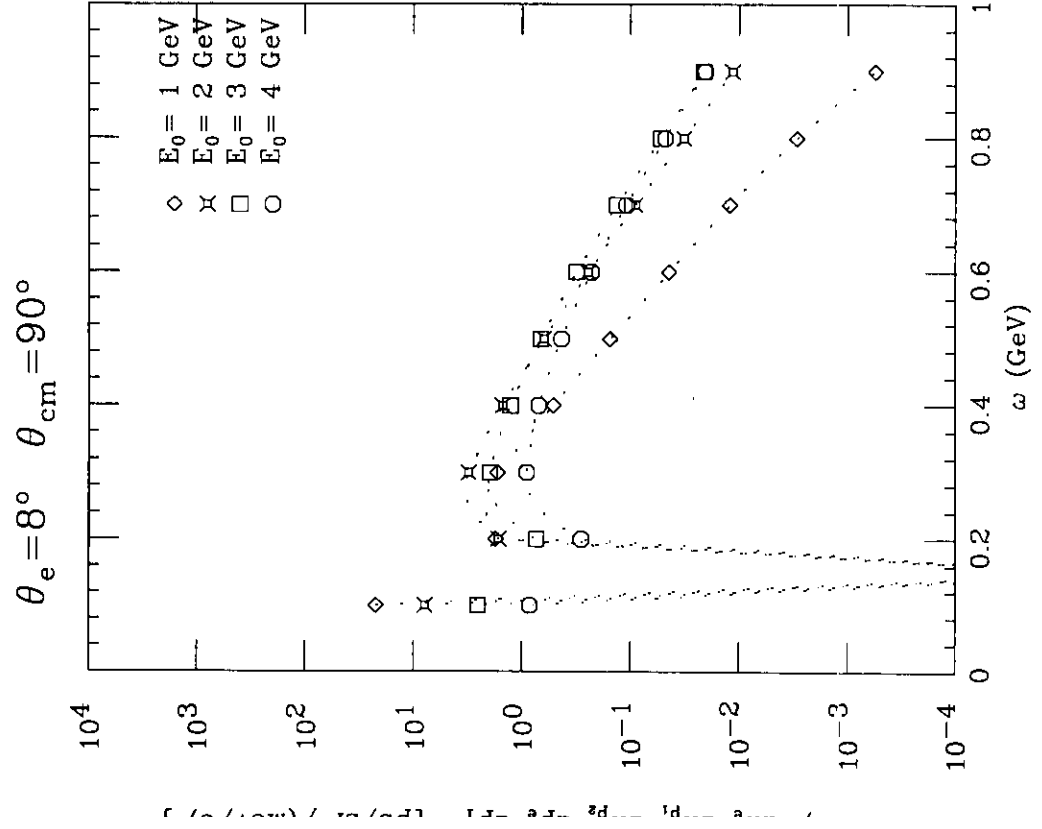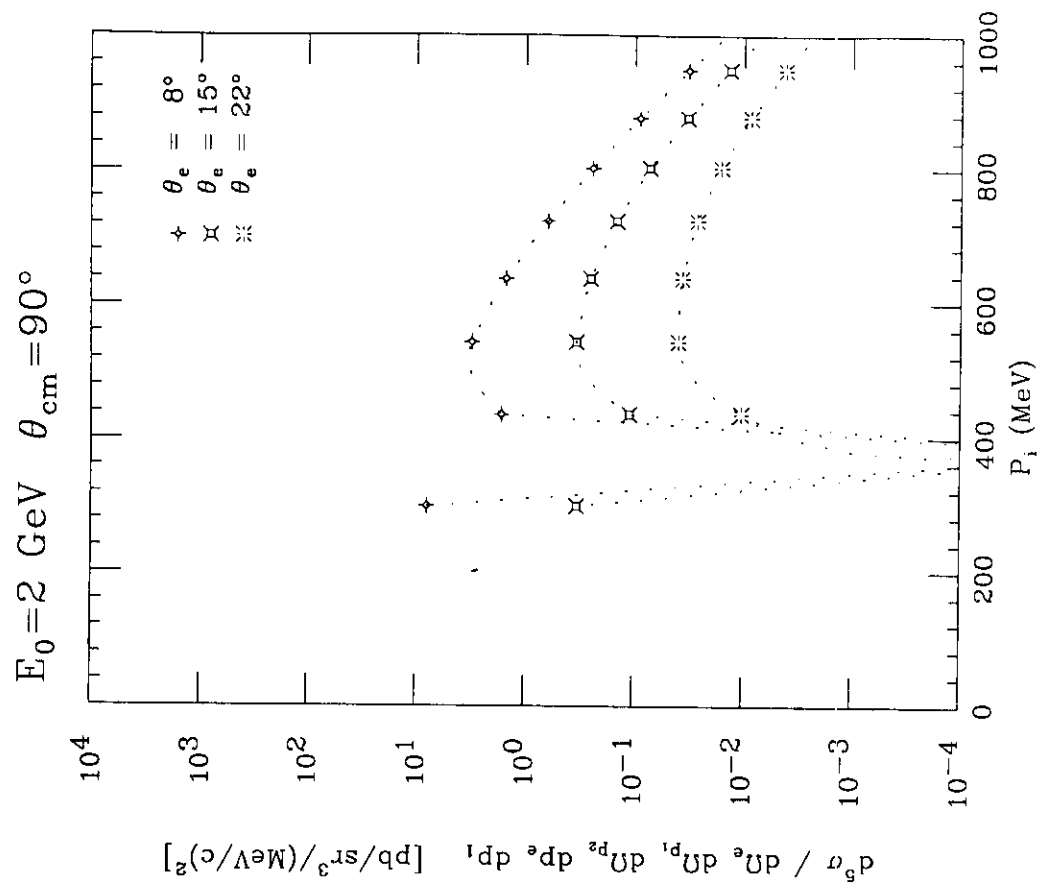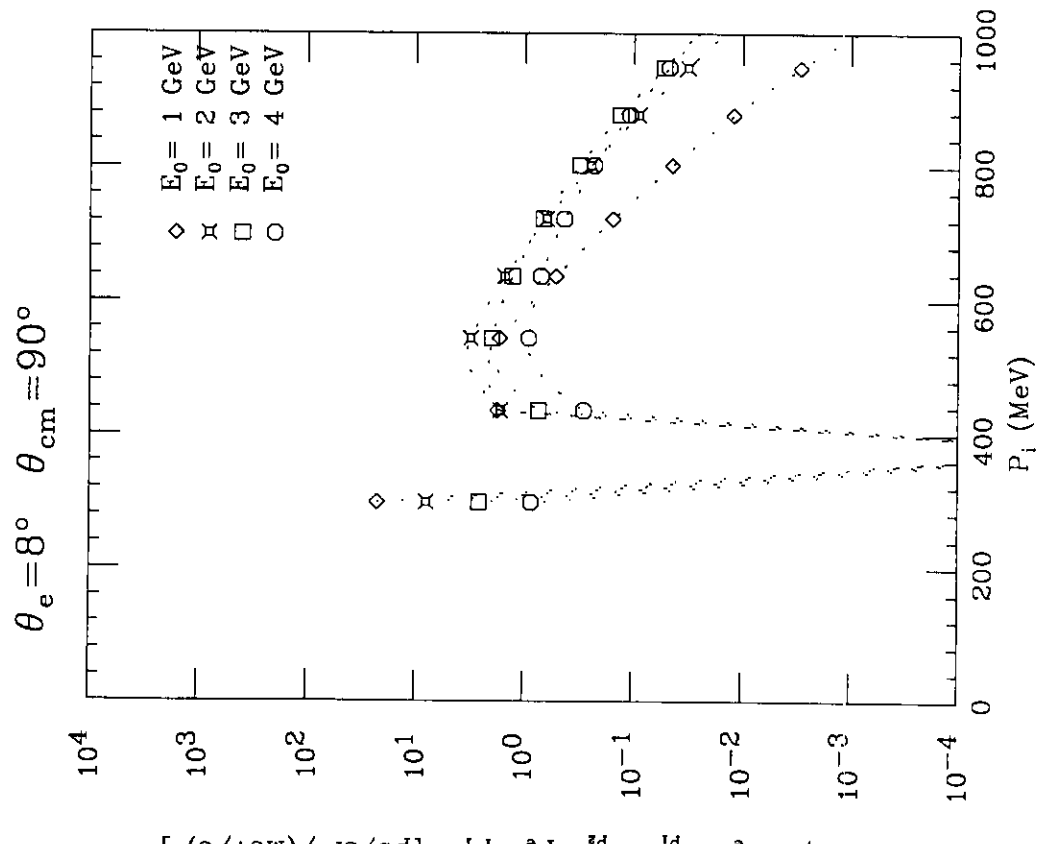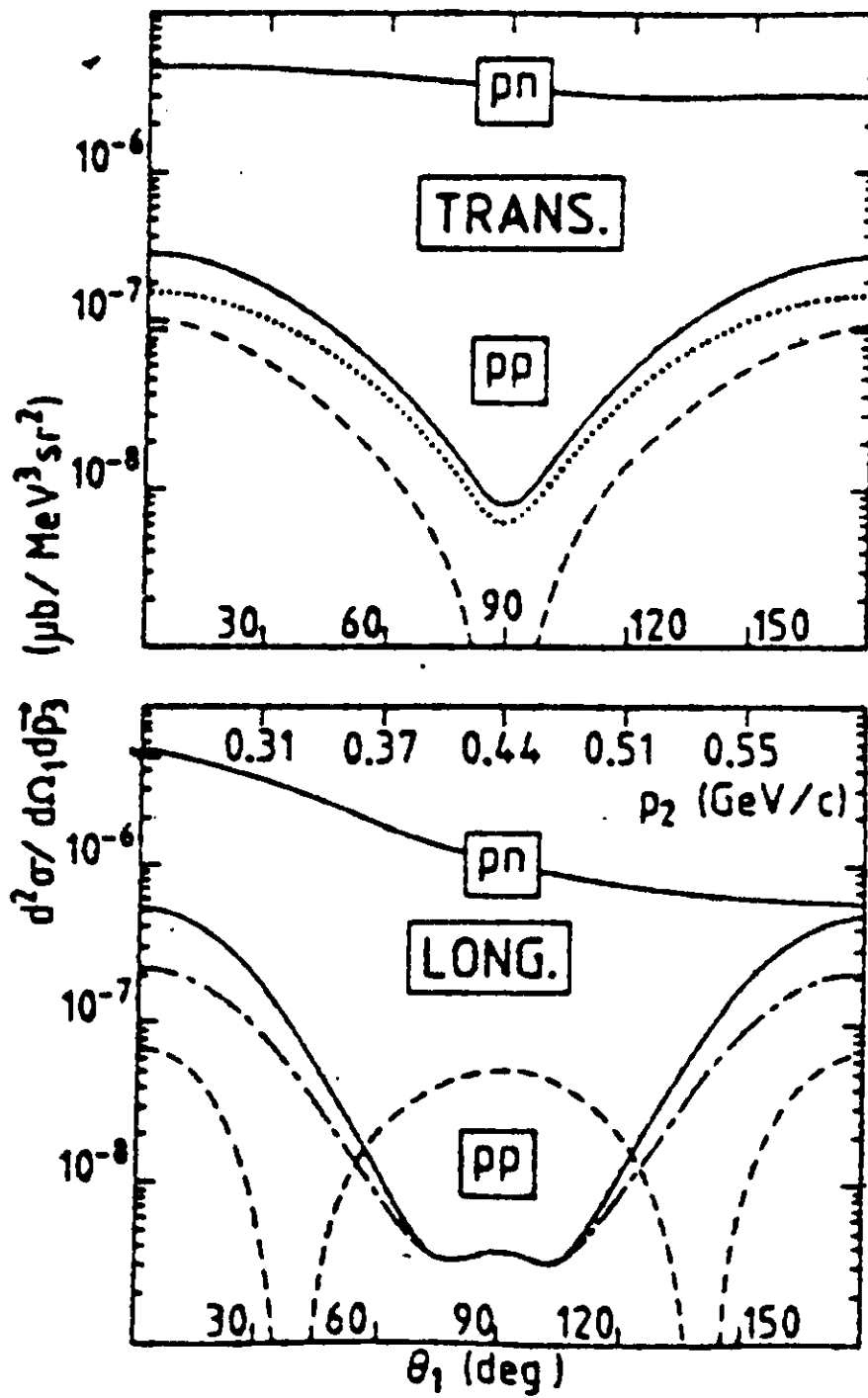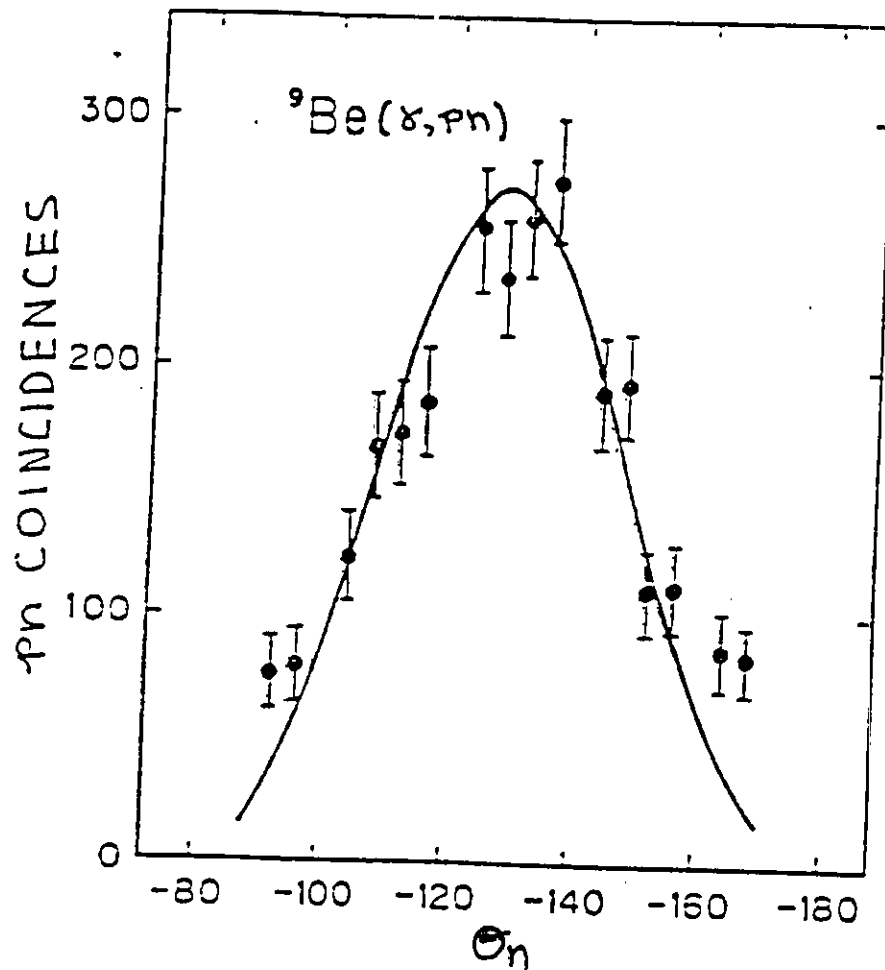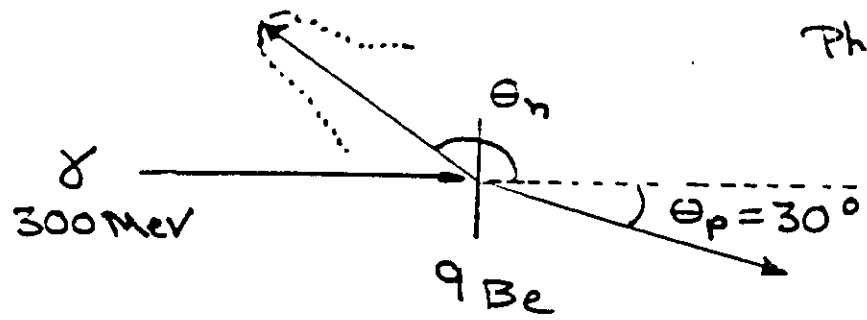
θ_n = NEUTRON LAB ANGLE (deg)

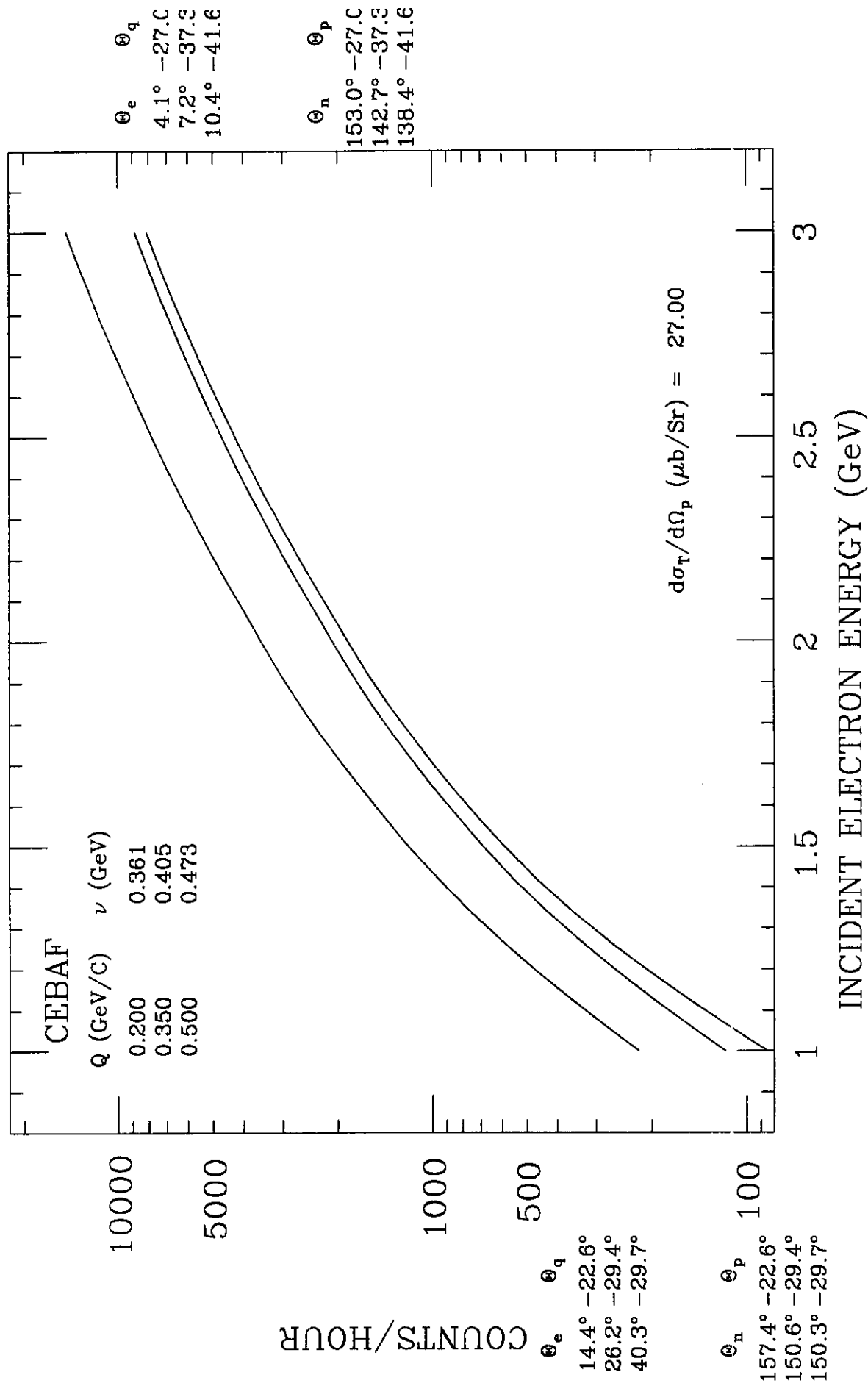$$\frac{d\sigma}{d\Omega_p} = \int \frac{d^2\sigma}{d\Omega_n}$$

$$= 35 \frac{\mu}{s}$$

$$E_\gamma = \omega = 300 \, MeV$$

$$P_p > 500 \frac{MeV}{c} \qquad \theta_p = 30°$$

$$P_n > 200 \frac{MeV}{c}$$

TARGET MASS (AMU) = 3.0   W (GeV) = 1.2

CEBAF

Q (GeV/C)	ν (GeV)
0.200	0.361
0.350	0.405
0.500	0.473

Θ_e	Θ_q
4.1°	−27.0
7.2°	−37.3
10.4°	−41.6

Θ_n	Θ_p
153.0°	−27.0
142.7°	−37.3
138.4°	−41.6

$d\sigma_T/d\Omega_p \ (\mu b/Sr) = 27.00$

INCIDENT ELECTRON ENERGY (GeV)

COUNTS/HOUR

Θ_e	Θ_q
14.4°	−22.6°
26.2°	−29.4°
40.3°	−29.7°

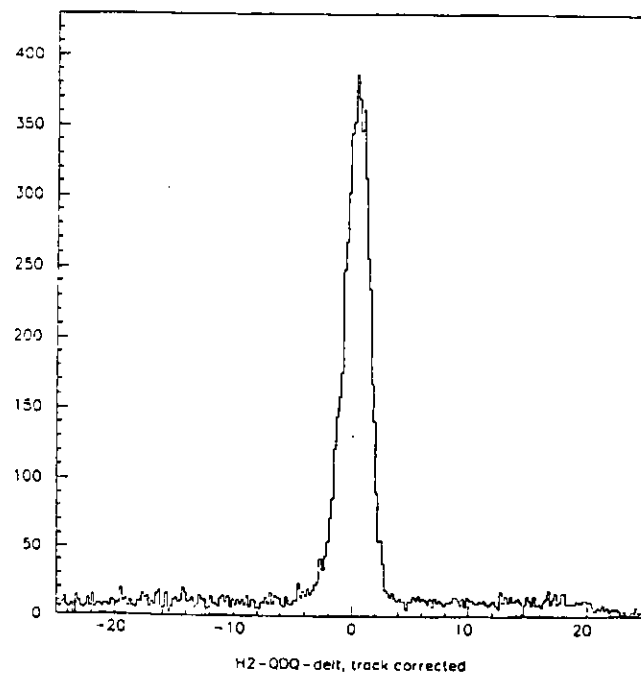| Θ_n	Θ_p
157.4°	−22.6°
150.6°	−29.4°
150.3°	−29.7°

t (mg/cm²) = 750.0 $\Delta\Omega_e$ (mSr) = 4.9 $\Delta\Omega_p$ (mSr) = 16.0 $\Delta\Omega_n$ (mSr) = 40.0 $\epsilon_n = 0.200$

I (μamps) = 20.0 $\Delta E' = 0.100 \times E_i$

Scintillator Hodoscope
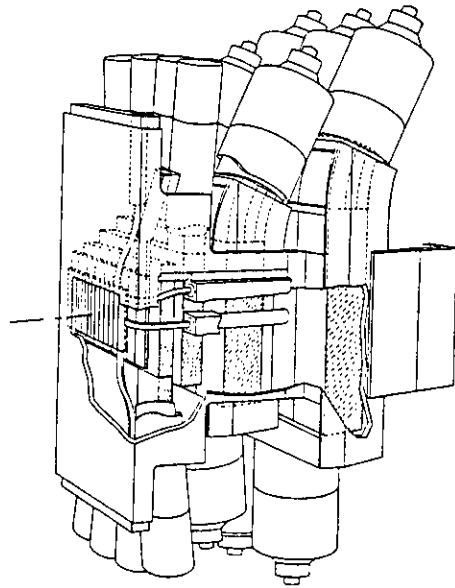
Timing Spectrum

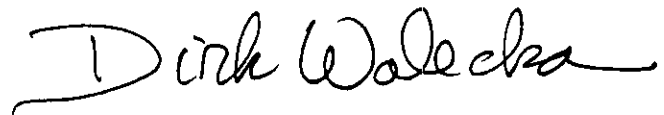H2-QDQ-delt, track corrected

Proposal Number: PR-89-030

Proposal Title: Two Nucleon Knockout Reactions on ^{3,4}He

Spokespersons/Contact Persons: M. Epstein, R. Lindgren, G. Lolos, Z-E Meziani

Proposal Status at CEBAF:

Deferral.

John Dirk Walecka
Scientific Director